




Article

Tracking Heme-Protein Interactions in Healthy and Pathological Human Serum in Native Conditions by Miniaturized FFF-Multidetetection

Valentina Marassi ^{1,2,*} , Stefano Giordani ^{1,†}, Pierluigi Reschiglian ^{1,2}, Barbara Roda ^{1,2}  and Andrea Zattoni ^{1,2,*} 

¹ Department of Chemistry G. Ciamician, University of Bologna, 40126 Bologna, Italy; stefano.giordani7@unibo.it (S.G.); pierluigi.reschiglian@unibo.it (P.R.); barbara.roda@unibo.it (B.R.)
² byFlow SRL, 40129 Bologna, Italy
 * Correspondence: valentina.marassi2@unibo.it (V.M.); andrea.zattoni@unibo.it (A.Z.)
 † These authors contributed equally to this work.

Abstract: The interaction of heme with blood serum proteins plays an important role in many physiological and pathological processes involving enzyme activity, gene expression and cell proliferation. The mechanisms underlying these interactions are; however, not yet fully understood. New analytical methods able to investigate protein-heme binding in native, biologically representative conditions are thus required. In this work, we present a method based on miniaturized, hollow-fiber flow field-flow fractionation with multiple spectrophotometric and light-scattering detection for size separation of high-abundance serum proteins and selective detection of heme-bound subpopulations. Heme is found to mainly interact with serum albumin, whereas a low amount also binds to other proteins such as IgM. The ability to bind heme in physiological conditions is also investigated for individual serum proteins. IgG is found unable to bind heme at clinically relevant concentrations. The proposed method allows separation, quantitation, and mass/size characterization of serum high-abundance proteins, providing information of heme-protein complex stability and preferred heme-clearing pathways. The same approach could be in perspective extended to the investigation of specific heme-antibody binding, and to further studies involving other molecules of pharmaceutical/clinical interest.

Keywords: serum-heme interactions; native separation; flow-field flow fractionation multidetetection; online characterization and quantification; hydrodynamic sorting; native study; protein binding



Citation: Marassi, V.; Giordani, S.; Reschiglian, P.; Roda, B.; Zattoni, A. Tracking Heme-Protein Interactions in Healthy and Pathological Human Serum in Native Conditions by Miniaturized FFF-Multidetetection. *Appl. Sci.* **2022**, *12*, 6762. <https://doi.org/10.3390/app12136762>

Academic Editor: Carlo Zamboni

Received: 28 May 2022

Accepted: 2 July 2022

Published: 4 July 2022

Publisher's Note: MDPI stays neutral with regard to jurisdictional claims in published maps and institutional affiliations.



Copyright: © 2022 by the authors. Licensee MDPI, Basel, Switzerland. This article is an open access article distributed under the terms and conditions of the Creative Commons Attribution (CC BY) license (<https://creativecommons.org/licenses/by/4.0/>).

1. Introduction

Heme is an iron-containing porphyrin of vital importance since it is involved in many key processes in the human organism. Proteins characterized by the presence of Heme as prosthetic group are called hemoproteins. Some of them, such as hemoglobin and myoglobin, use it for oxygen transport, electron transport, energy generation, and chemical transformation (in cytochromes). In catalases and peroxidases, heme functions in hydrogen peroxide inactivation or activation, respectively, and in tryptophan pyrrolase, it catalyzes the oxidation of tryptophan [1]. Heme is also involved in other important enzyme systems such as cyclooxygenase and nitric-oxide synthase [2]. Heme however does not only function as a prosthetic group: in particular, it is involved in the control of gene expression at almost all levels by regulating transcription, mRNA stability, splicing, protein synthesis, and post-translational modification [3]. This is possible due to heme-responsive elements located in the genes and the mammalian transcription repressor, Bach1 [4]. In addition, heme regulates differentiation and proliferation of various cell types [5]. Heme that is not bound to proteins is called “labile heme pool”; it is originated from newly synthesized heme that has not yet been incorporated into hemoproteins, or heme that has been released from hemoproteins under oxidative conditions.

An excess of free heme is toxic for the organism. High levels of redox-active iron (contained in heme) can catalyze the formation of Reactive Oxygen Species (ROS). ROS damage lipid membranes, proteins, nucleic acids, activate cell signaling pathways and oxidant-sensitive, proinflammatory transcription factors, alter protein expression, and perturb membrane channels [6,7]. Due to its lipophilic nature, heme is able to intercalate in the lipidic membrane causing cellular lysis [8]. Finally, heme is strongly pro-inflammatory since it induces the recruitment of leukocytes and consumes nitric oxide, thus impairing vascular function. The production of ROS and the membrane damage caused directly and indirectly by heme make it a strong hemolytic agent. Several pathological conditions are associated with hemolysis, including sickle cell anemia, thalassemia, malaria, paroxysmal nocturnal hemoglobinuria, etc. [9]. Other vascular diseases caused by a detrimental effect of heme on the vessel wall are atherosclerosis and vascular calcifications [10].

Due to free heme toxicity, blood serum is equipped with mechanisms to prevent extracellular heme toxicity. Among them, a key function is covered by the soluble scavengers of free hemoglobin and heme, Haptoglobin (Hp) [11] and Hemopexin (Hx) [8], respectively. Hp acts on the dangerous free hemoglobin released by hemolysis processes by capturing it and generating a complex which is sent to the reticulo-endothelial system for its elimination [12]. When the buffering capacity of plasma Hp is exceeded, hemoglobin is quickly oxidized to methemoglobin, which releases free heme [13]. Heme is then bound by Hx. Hx is a 57-kDa acute phase plasma glycoprotein, able to bind an equimolar amount of heme and to deliver it to hepatocytes where the heme-Hx complex is internalized by receptors LRP 1 (LDL receptor-related protein 1) mediated endocytosis [5]. However, when hemolysis levels are too high or comorbidities reduce the bioavailability of hemopexin, other proteins act as scavenging heme agents, namely serum albumin (SA), LDL, HDL, and Immunoglobulins [14]. The interest upon heme-protein affinity is not only correlated to restoring homeostasis properties. It has been observed that heme-exposed IgGs, following an appropriate incubation procedure, can exhibit new and promising properties (such as polireactivity), and with this regard some of the serum immunoglobulins interact with heme [15]. Literature describing what happens during these incubation procedures is very diverse. Some studies suggest that heme, due to its pro-ox nature, induces chemical modification of IgGs without the formation of a stable complex [16,17]. Others instead showed the existence of binding, and formation of stable complexes, between heme and antibodies [14,18,19]. However in each of these studies, the drawback of having simultaneous bound and unbound heme led to difficult quantification and lab-heavy functionalization steps (immobilization, derivatization). Some approaches to determine biomolecule-biomolecule interactions exploit coimmunoprecipitation [18,19]. Others use imaging such as atomic force microscopy, based on force spectroscopy (AFM-FS) [20,21], magnetic tweezers and dynamic light scattering [22,23]. Energy transfer such as Förster resonance energy transfer (FRET) [24,25], Bioluminescence resonance energy transfer (BRET) [26] and fluorescence cross-correlation spectroscopy (FCCS) [27,28] are also employed. In the case of serum-heme interactions, it is to be noted that the experimental difficulties are numerous, and the matrix is very complex. Consequently, all the experiments conducted up to date aimed at understanding the involvement of serum protein for heme scavenging were carried out in an isolated and compartmentalized way, which on one hand facilitates recognition, but on the other hand represent only a partial result that does not necessary fully translate to the real matrix or the physiological state [29–32]. To examine heme-protein interactions in a more representative scenario, where proteins are simultaneously present in the matrix (in their biological concentrations) and can both concur and compete for binding, it is necessary to develop a detection system that simplifies the sample while preserving its native state. In previous works the ability of F4 (Flow field-flow fractionation) and its miniaturized version HF5 (hollow-fiber F4) platforms to perform this task was demonstrated [33–35]. F4 (Flow Field Flow Fractionation) techniques are a class of analytical techniques that separate analytes based on their hydrodynamic radius due to the combined action of a laminar flow of a carrier solution, named elution flow, and a flow

applied orthogonally to the elution flow, named cross flow. Cross flow drives the analytes into different regions of the laminar flow, resulting in different retention times. Based on the shape of the channel and how the perpendicular flow is applied, different variants of F4 can be defined. HF5 represents the miniaturized version of the common Asymmetrical F4 (AF4) subclass [36,37]. As the name suggests, the separation device consists in a hollow fiber in which the main flow entering the fiber is split into two components: a flow coaxial to the fiber (the laminar parabolic flow) and a radial flow (the crossflow), as schematized in [38]. When compared to other size-based separation methods, F4 techniques show broader size separation range (from 1 nm up to $>1\ \mu\text{m}$) and higher flexibility, in terms of mobile phases used (ability to work in native conditions). Moreover, working with an empty channel prevents destruction of the aggregates due to their interaction with the stationary phase, allowing a better evaluation of conjugates formation [39–43]. HF5, in addition, provides the highest resolutions of the F4 variants, allows to work with lower volumes (both of sample and mobile phase), and the separation device can work in a disposable mode [44]. Thanks to these outstanding advantages, systems derived from the hyphenation of HF5 to uncorrelated detectors such as multi-angle light scattering (MALS), UV/vis Absorption and fluorescence, and Refractive Index have been exploited for the separation and characterization (mass, size and spectroscopic properties) of numerous samples such as biocompatible nanoparticles [45–47], biological samples of varying complexity [48–50], and other products of pharmaceutical interest [37,51,52].

Within this framework, the aim of this work was the study of the interactions between heme and serum components (like SA and IgG) in a real-life environment. The first step was to successfully separate serum into subcomponents (mainly SA, IgG, IgM and lipoproteins) within the separation method, to correctly identify heme-protein interactions. Then, increasing heme amounts were added to a native serum sample and an IgG-enriched serum sample also simulating an inflammatory response to monitor simultaneous protein-heme interactions [53]. The unbound heme is filtered away during the focus step [38,44,45] of the analysis, which acts as a filtration step, thus only the protein-bound heme fraction is selectively detected. The products of heme-protein interaction, along with the other serum components, were separated and evaluated with an HF5 platform coupled with UV/vis and MALS detectors. These detectors respectively allowed monitoring of protein, and heme-protein complexes through their typical absorption wavelengths (280 nm and 405 nm, respectively) and yielded mass and size of the serum components separated through the fiber. PBS was chosen as mobile phase to simulate a physiological environment. Our results confirmed the excellent ability of HF5-multidetector to separate serum components and distinguish what components are affected by the presence of free heme. Compared to pre-existing literature, these separations and incubation were performed injecting undiluted serum. The amount of sample required for the analysis was extremely low, due to the exploitation of the miniaturized F4 variant, and the analysis time being below 30 min for each analysis. In agreement with pre-existing “single component” studies [29–32], we observed that serum’s heme-scavenging power is mainly represented by SA and Hx, and to a much lower degree by some immunoglobulins. IgG scavenging contributions in the presence of clinically relevant free heme levels (5–40 μM) can instead be considered negligible. Moreover, we showed that our platform can be exploited for the non-destructive separation and collection of different heme-serum fractions which may undergo further analysis. The setup allows for fast and sensitive detection and potential quantitation of parameters linked to pathological conditions, in terms of haemolysis and inflammation through direct detection of diagnostic signals (heme or other probe molecules) or peak changes (IgG, SA). Such an approach could also be translated towards the study of selective heme-antibody binding to investigate specific interactions at the native state, preserving spatial arrangements.

2. Materials and Methods

2.1. Heme-Serum and Heme-Protein Preparations

Human serum albumin and IgG standard solutions were prepared starting from lyophilized proteins and resuspending them in PBS; human SA (HSA) and IgG were commercially obtained (Merck Sigma Aldrich, Darmstadt, Germany). A 10 mM heme (Sigma Aldrich, Darmstadt, Germany) stock solution was prepared in 10 mM NaOH and used to spike serum and protein solutions. Serum was collected from 4 healthy volunteers and pooled to account for individual variability. To inject unmodified serum or heme-spiked serum, a set of samples was prepared via addition of PBS (serum) or heme (spiked serum) to whole serum to obtain final heme concentrations of 0, 5, 10, 20, 40 μ M. To prepare IgG-spiked serum, whole serum was spiked with IgG to obtain final IgG concentrations of 20, 25 and 30 mg/mL. These solutions were then spiked with heme or PBS to achieve the same final heme concentration (20 μ M).

Standard HSA and IgG injections were performed starting from solutions at the same concentration found in serum (600 and 70 μ M, respectively). The same procedure used for serum was performed with protein solutions to monitor individual interactions with heme. The injection volume was 0.25 μ L for all samples.

2.2. HF5-Multidetetection

HF5 analyses were performed using an Agilent 1200 HPLC system (Agilent Technologies, Santa Clara, CA, USA) consisting of a degasser, an isocratic pump, with an Agilent 1100 DAD UV/Vis spectrophotometer combined with an Eclipse[®] DUALTEC separation system (Wyatt Technology Europe, Dernbach, Germany). The HF5 channels used for the experimental section were standard cartridges containing a 17 cm long hollow fiber, commercially available. The fiber was a type FUS 0181 polyethersulfone (PES) fiber, available from Microdyn-Nadir (Wiesbaden, Germany) with the following characteristics: 0.8 mm inner diameter, 1.3 mm outer diameter, and 10 kDa Mw cut-off, corresponding to an average pore diameter of 5 nm. Channel pressure limit was set at 20 bar. The ChemStation version B.04.02 (Agilent Technologies, Santa Clara, CA, USA) data system for Agilent instrumentation was used to set and control the instrumentation and method parameters. An 18-angle light scattering detector model DAWN HELEOS (Wyatt Technology Corporation, Santa Barbara, CA, USA), operating at 658 nm wavelength, was used to measure the light scattering signal from particles in solution. ASTRA[®] software version 6.1.7 (Wyatt Technology Corporation, Santa Barbara, CA, USA) was used to handle signals from the detectors (MALS and UV) and to compute the sample root mean square radius of gyration (R_g) values. An HF5 method is composed of four steps: focus, focus-injection, elution and elution-injection. During focus the mobile phase enters from both inlet and outlet and stabilizes; during focus-injection, the flow settings remain unvaried while the sample is introduced into the channel through the inlet and focused in a narrow band. Then, in the elution step, the flow of mobile phase enters the channel inlet and part of it comes out transversely (cross-flow, V_x), while the rest (channel flow, V_c) reaches the detectors; lastly, during elution-injection, no cross-flow is applied allowing for any remaining sample inside the channel to be released; also, the flow is redirected in the injection line as well to clean it before the next injection. A non-separative method can be used to evaluate sample recovery. In particular, a Flow Injection Analysis (FIA), i.e., a run with zero focus flow, zero crossflow, allows for total recovery of the sample, including molecules and particles smaller than the membrane's cutoff. By comparing areas between a FIA and a separation method, recovery % is obtained. Analyses were carried out in isotonic, pH 7.4 PBS as mobile phase. The flow rate program of the separation method was set up as follows: inject flow of 0.20 mL/min, a focus flow of 0.80 mL/min (4 min), an initial crossflow of 0.40 mL/min decreasing to 0.2 (16 min), an isocratic step (6 min) and a detector flow of 0.40 mL/min. MALS analysis allows for the determination of particle R_g by the mass distribution within the particle. Knowing the absorptivity (ϵ) and the specific refractive index increment (dn/dc) for the eluted sample (ϵ values were set as 0.667 mL/(mg·cm) for BSA and 1.37 for IgGs, while a generic 1 value

was used for later eluted proteins [54]; dn/dc was set as 0.185 mL/g), molar mass can be calculated from R_g . Molar mass and R_g distributions can be combined into a scaling exponent ν , i.e., the slope in a double logarithmic $\log MM$ vs. $\log R_g$ plot, which describes the conformation of the molecules in solution. It is theoretically defined as $\nu = 0.33$ for spheres, $\nu = 0.5$ – 0.6 for random-coils, and $\nu \sim 1$ for rod-like structures [48]. The total method duration was 28 min. Method precision was assessed both on retention times and on signal intensity by performing three independent replicates for serum and protein standards. The limit of quantification (LOQ) was calculated as the injected amount (pmol) at which the signal is 10 times the signal noise of the baseline. All graphs were elaborated in GraphPad Prism.

3. Results and Discussion

3.1. HF5 Separation of Serum

Blood serum is a complex sample, containing small molecules, proteins, lipoproteins and micelles and other particles; a simplification is necessary when monitoring selected interactions such as those with free heme. At the same time, it is crucial to preserve the sample native state, to avoid alterations in behavior. The developed method was optimized with the aim of separating serum in its main size components in the shortest analysis time, which was achieved by a combination of isocratic and gradient cross-flow, using isotonic PBS (pH = 7.4) as mobile phase. Recovery, calculated in triplicate from the UV/vis signal at 280 nm, was evaluated for serum, HSA and IgG; in all cases, we obtained quantitative recovery (>99.9%). On the contrary, recovery after injection of free heme was 0% as expected, confirming that only heme binding to proteins was selectively detected, while free heme was effectively filtrated through the hollow fiber pores during the focusing step (see Supplementary Data, Figures S1 and S2). The limit of quantification (LoQ), which could be calculated for reference proteins HSA and IgG, corresponded to 0.0012 pmol and 0.0003 pmol, respectively. The total analysis time resulted to be below 30 min.

Serum analysis yielded four main bands, peaking at 8.4, 11.0, 15.3 and 20.3 min, respectively (Figure 1a). Absorption intensity decreases from the first to the last peak, while light scattering (which is also sensitive to size) increased as expected, confirming the size differences between the four populations. Characterization and identification of these bands is easily accessible when using HF5-multidetector, since the combination of a concentration detector (UV) and light scattering (MALS) allows for the direct determination of size and molar mass of the eluting species. In this regard, HF5 (and more broadly FFF) with multidetection can offer a standalone technique.

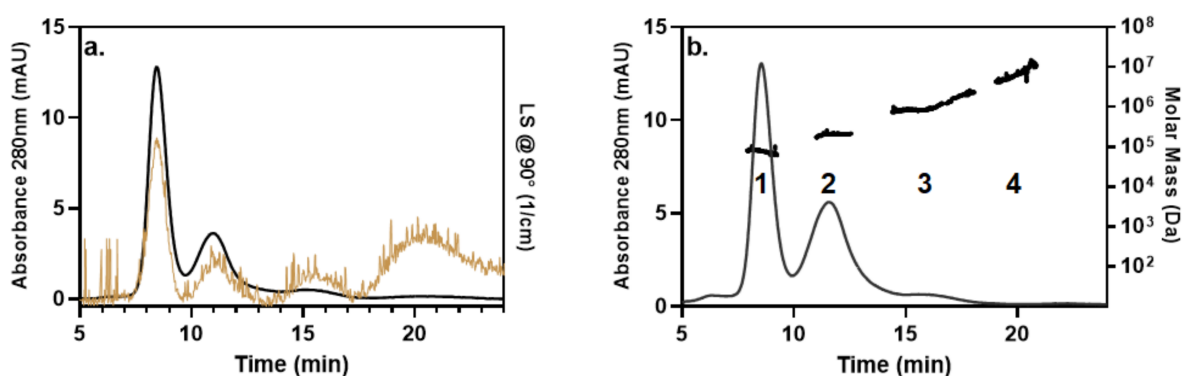


Figure 1. Separation profile of whole serum. (a) UV @280 nm (black trace) and LS@90° (yellow trace). (b) UV profile and Molar Mass overlay (black distributions) of the four bands.

For what concerns peak attribution, two classes of components can be distinguished, proteins and lipoproteins. Proteins have the strongest absorption at 280 nm, while lipoproteins assemble into tridimensional structures.

The average molar mass values calculated for the four bands (Figure 1b), using UV absorption at 280 nm as concentration source, were 7.1 ($\pm 12\%$) kDa, 162 ($\pm 16\%$) kDa, 990 ($\pm 25\%$) kDa, 1.6 ($\pm 8.5\%$) MDa. Therefore, the four bands could be attributed to i. mainly BSA (and Haemopexin, which has a similar molar mass) and coeluted HDL [34], ii. IgG (namely 150 kDa) with IgD and IgE (180 and 200 kDa) tailing into IgA (320 kDa), iii. IgM and possible further aggregates of smaller immunoglobulins, iv. LDL and VLDL particles (measured R_g : 14–35 nm), with a scaling exponent $\nu = 0.89$, compatible with a non-spherical morphology where mass is distributed on the surface of a core-shell discoidal particle. This is in line with literature concerning serum and plasma characterization in similar setups [33,55].

The confirmation of the nature of the first two bands also comes from independent injections of standard proteins, such as HSA and IgG with the same method. These two proteins were chosen as example since they together represent the most part of serum protein content and are the most reported in heme binding studies. In the case of HSA, aggregates are also present in the standard sample (Figure 2, blue trace), and the retention time of the monomer corresponds to band 1 maximum. In the case of IgG (Figure 2, green trace), there are no aggregates detected and retention time is in line with band 2. The injection of different amounts of standard protein and following calibration of their content in serum can also act as rapid quantitation of albumin and immunoglobulin and give immediate feedback on healthy/inflammatory/disease conditions.

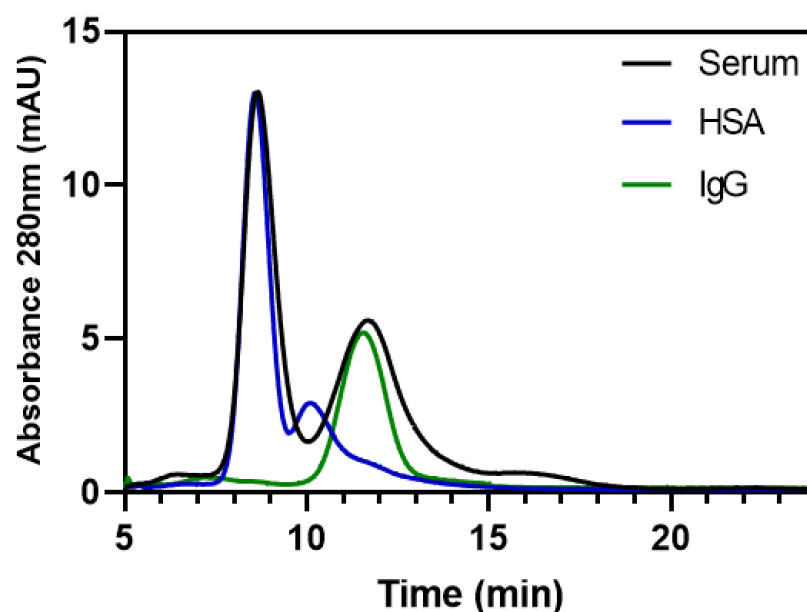


Figure 2. Separation profile of whole serum (black), HSA (blue) and IgG under the same analysis conditions.

3.2. Serum—Heme Binding Study

After identification of serum components, the following concern was the specificity of detection: the selectivity towards bound heme was already confirmed with a 0% recovery of free heme (Supplementary Data, Figure S2), but univocal detection also needed confirmation. In Figure 3 the differential absorption of HSA, serum, and IgG at 280 and 405 nm (heme absorption maximum) is shown. All three samples absorb strongly at 280 nm but show no absorption at 405 nm. The lack of signal at 405 nm found for serum confirms that this setup can allow to work in a ‘single experiment’ setting, where individual proteins can be used for further detailed studies after a general behaviour is observed. In fact, serum itself, sorted in its component, is a clear negative control and any difference in heme binding can be promptly and selectively detected.

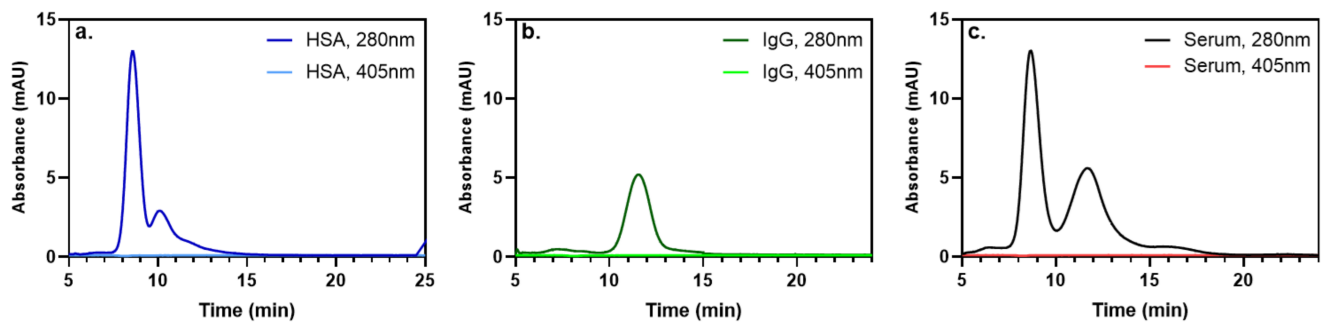


Figure 3. Differential absorption at 280 nm and 405 nm for (a) HSA (b) IgG and (c) serum.

The same amount of serum was treated with increasing amounts of heme to obtain heme final concentrations of 5, 10, 20, 40 μM and analyzed with HF5-mutidetection (Figure 4). As the concentration of heme increased, it was possible to observe the formation of an intense peak at 405 nm reflecting the retention time of band 1.

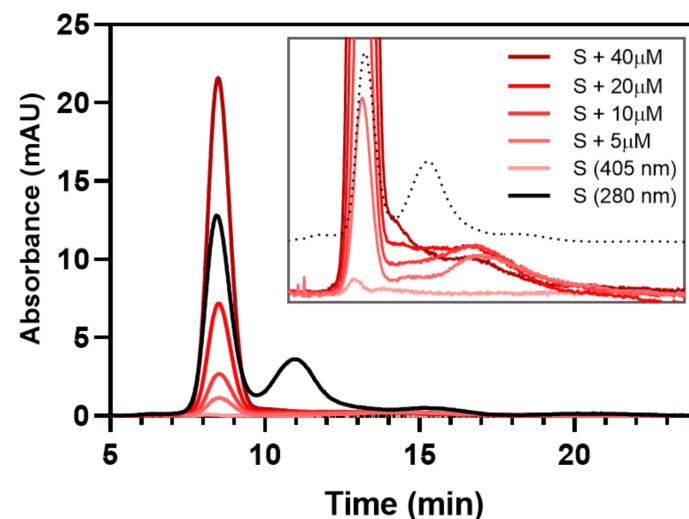


Figure 4. Overlay of absorption at 405 nm of serum treated with increasing heme concentrations (5–10–20–40 μM). Black trace: serum profile at 280 nm. Inset: zoom of the fractograms overlay to observe low signals at the tail of band 1 and at 13–17 min.

The interaction between heme and band 1 was predominant, while a very low signal could be found in band 1's tail, and at around 13 min tailing into band 3 (Figure 4, inset). These signals can be attributed to SA aggregates, hemopexin, and HDL [56–58] and other type of immunoglobulins such as IgA and IgM [59,60]. Interestingly, no interaction was observed in correspondence of band 2, attributed to IgG. Though a few works reporting interactions between heme and immunoglobulins are found in literature, it is important to notice that they do not regard interaction studies in physiological conditions and concern specific classes of antibodies, often specifically made [61]. On the contrary, the formation of stable complexes between blood proteins and heme is not fully understood and this setup can contribute to increase the knowledge on preferred heme-clearing pathways.

As confirmation and to correctly interpret the interactions between SA and heme, mixtures of SA or IgG and the same amount of heme previously employed were also analyzed. In the case of SA, interaction was not only confirmed, but also yielded peak integrals identical to what was found in correspondence of band 1 (Figure 5a). In this case, as SA dimer and oligomers were also present, it was possible to notice how all aggregated states of SA interacted with heme at the same time and at all concentrations.

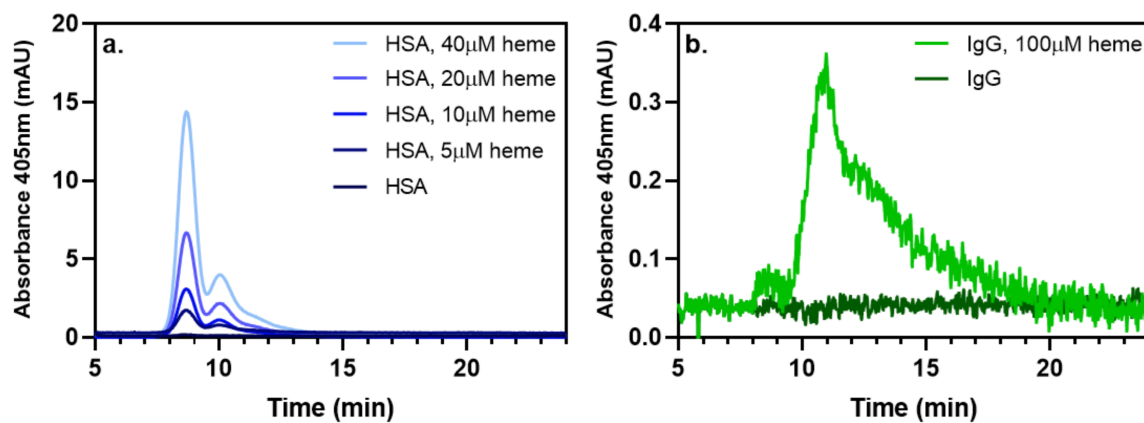


Figure 5. (a) Overlay of absorption at 405 nm of SA treated with increasing heme concentrations (5–10–20–40 μ M). (b) overlay of absorption at 405 nm for untreated IgG (dark green) and IgG treated with 100 μ M heme (light green).

Instead, for what concerns IgG, no signal at 405 nm was detected at the tested concentrations and thus we increased the amount of heme until a visible signal was detectable; this only happened when final heme concentration reached 100 μ M (Figure 5b), which is beyond clinical interest [62].

Lastly, and as an additional investigation on the possible competition and binding equilibria in serum, we also searched for interactions between IgG-enriched serum and heme; in fact, some literature reports IgG-heme binding in case of the opposite imbalance to that shown above [32].

Serum was enriched to reach a final IgG concentration of 20, 25 and 30 μ M, in the range of moderate-to-severe clinical conditions, to also simulate co-morbidity to hemolytic diseases. Then, heme was added to the sample which was submitted to HF5-multidetector analysis. In Figure 6, the serum profiles at 280 nm (grey traces), reflecting the increase in IgG content, and at 405 nm (20 μ M heme mixes shown as representative example, red traces) are overlaid.

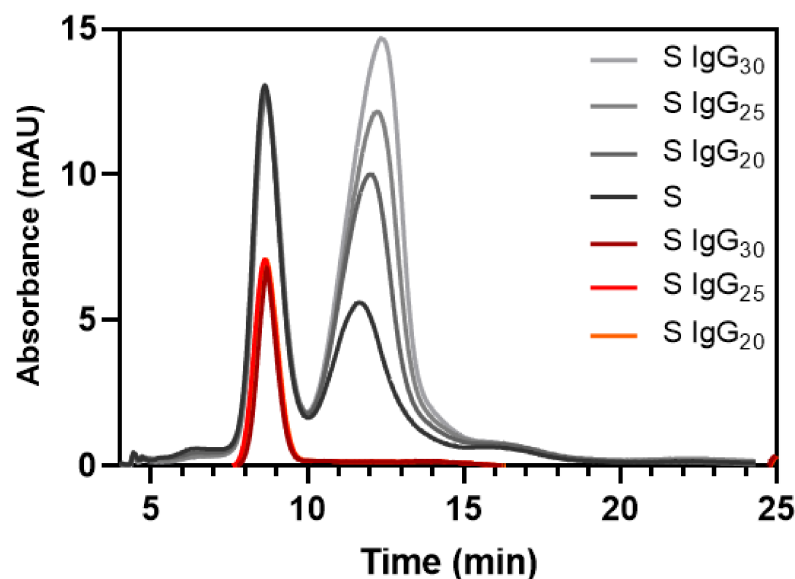


Figure 6. Overlay of absorption at 280 nm (grey) of IgG-enriched serum treated with 20 μ M heme. Red trace: absorption at 405 nm reflecting bound heme presence.

Band 2 increased in absorption at 280 nm with increasing IgG content, as expected from peak attribution; indeed, as mentioned above, this approach can simultaneously detect

variation in patients' conditions which modify serum proteins concentration. However, no additional signal is detected at 405 nm, indicating that even in the case of a stronger concentration imbalance between heme and IgG, the latter is not prone to the formation of a bound system, and SA is the main heme scavenging protein through binding as both monomer and aggregates.

4. Conclusions

In this work, we devised a method based on miniaturized F4-multidetector to size-separate blood serum into four components (SA and size equivalents, IgG and 200–300 kDa immunoglobulins, IgM, lipoprotein particles), in order to study the interactions between heme and each subpopulation in a native and representative state. The experiments were carried out in PBS and required a short analysis time (<30 min) and very little sample injection volumes. As low as 0.5 μ L of serum could be injected, and the presence of bound heme could be selectively monitored thanks to the removal of free heme during the method's focusing step. The main interacting protein was found to be serum albumin, while a low amount of heme also bound to other proteins such as IgM. The ability/inability to bind heme in physiological conditions was also verified individually for SA and IgG, the latter being incapable to bind heme at clinically relevant concentrations. To simulate co-morbidity and explore different concentration equilibria and competitions, we also employed an IgG-enriched serum, yielding the same results. This approach proved to be extremely information-rich, since it allows for mass and size characterization, subcomponent separation and monitoring of deviations of the concentration of serum's most abundant proteins. Since the formation of stable complexes between blood proteins and heme is not fully understood, this setup can contribute to increase the knowledge on preferred heme-clearing pathways. Moreover, this approach serves also as a proof-of-concept for further studies selectively monitoring other small molecules and probes of clinical/pharmaceutical interest. This is particularly relevant for complex samples such as serum, since it preserves native conditions and avoids recurring to time and lab-heavy processing steps. Lastly, this approach could also be translated towards the study of selective heme-antibody binding to investigate specific interactions at the native state, preserving spatial arrangements.

Supplementary Materials: The following supporting information can be downloaded at: <https://www.mdpi.com/article/10.3390/app12136762/s1>, Figure S1: platform schematics and method output; Figure S2: Negative control of heme alone in in HF5-multidetector.

Author Contributions: Conceptualization, V.M., A.Z., S.G. and B.R.; Data curation, S.G.; Funding acquisition, A.Z. and P.R.; Investigation, V.M. and S.G.; Methodology, V.M., S.G., A.Z., P.R. and B.R.; Supervision, A.Z. and V.M.; Writing—original draft, V.M., A.Z. and S.G.; Writing—review and editing, V.M., S.G., A.Z., P.R. and B.R. All authors have read and agreed to the published version of the manuscript.

Funding: This research received no external funding.

Institutional Review Board Statement: Not applicable.

Informed Consent Statement: Not applicable.

Conflicts of Interest: V.M., B.R., P.R. and A.Z. are associates of the academic spinoff company byFlow SRL (Bologna, Italy). The company mission includes know-how transfer, development, and application of novel technologies and methodologies for the analysis and characterization of samples of nano-biotechnological interest.

References

1. Kumar, S.; Bandyopadhyay, U. Free heme toxicity and its detoxification systems in human. *Toxicol. Lett.* **2005**, *157*, 175–188. [[CrossRef](#)] [[PubMed](#)]
2. Seed, M.P.; Willoughby, D.A. COX-2, HO NO! Cyclooxygenase-2, heme oxygenase and nitric oxide synthase: Their role and interactions in inflammation. BIRAs Symposium, Saint Bartholomew's Hospital, London, 26 April 1996. *Inflamm. Res.* **1997**, *46*, 279–281. [[CrossRef](#)] [[PubMed](#)]

3. Ponka, P. Cell biology of heme. *Am. J. Med. Sci.* **1999**, *318*, 241–256. [[CrossRef](#)]
4. Ogawa, K.; Sun, J.; Taketani, S.; Nakajima, O.; Nishitani, C.; Sassa, S.; Hayashi, N.; Yamamoto, M.; Shibahara, S.; Fujita, H.; et al. Heme mediates derepression of Maf recognition element through direct binding to transcription repressor Bach1. *EMBO J.* **2001**, *20*, 2835–2843. [[CrossRef](#)] [[PubMed](#)]
5. Chiabrando, D.; Vinchi, F.; Fiorito, V.; Mercurio, S.; Tolosano, E. Heme in pathophysiology: A matter of scavenging, metabolism and trafficking across cell membranes. *Front. Pharmacol.* **2014**, *5*, 61. [[CrossRef](#)]
6. Vercellotti, G.M.; Balla, G.; Balla, J.; Nath, K.; Eaton, J.W.; Jacob, H.S. Heme and the vasculature: An oxidative hazard that induces antioxidant defenses in the endothelium. *Artif. Cells Blood Substit. Immobil. Biotechnol.* **1994**, *22*, 207–213. [[CrossRef](#)]
7. Jeney, V.; Balla, J.; Yachie, A.; Varga, Z.; Vercellotti, G.M.; Eaton, J.W.; Balla, G. Pro-oxidant and cytotoxic effects of circulating heme. *Blood* **2002**, *100*, 879–887. [[CrossRef](#)]
8. Tolosano, E.; Fagoonee, S.; Morello, N.; Vinchi, F.; Fiorito, V. Heme scavenging and the other facets of hemopexin. *Antioxid. Redox Signal.* **2010**, *12*, 305–320. [[CrossRef](#)]
9. Gozzelino, R.; Jeney, V.; Soares, M.P. Mechanisms of cell protection by heme oxygenase-1. *Annu. Rev. Pharmacol. Toxicol.* **2010**, *50*, 323–354. [[CrossRef](#)]
10. Nagy, E.; Eaton, J.W.; Jeney, V.; Soares, M.P.; Varga, Z.; Galajda, Z.; Szentmiklósi, J.; Méhes, G.; Csonka, T.; Smith, A.; et al. Red cells, hemoglobin, heme, iron, and atherogenesis. *Arterioscler. Thromb. Vasc. Biol.* **2010**, *30*, 1347–1353. [[CrossRef](#)]
11. Schaer, D.J.; Buehler, P.W. Cell-free hemoglobin and its scavenger proteins: New disease models leading the way to targeted therapies. *Cold Spring Harb. Perspect. Med.* **2013**, *3*, a013433. [[CrossRef](#)] [[PubMed](#)]
12. Jamwal, M.; Sharma, P.; Das, R. Laboratory Approach to Hemolytic Anemia. *Indian J. Pediatrics* **2020**, *87*, 66–74. [[CrossRef](#)] [[PubMed](#)]
13. Ascenzi, P.; Bocedi, A.; Visca, P.; Altruda, F.; Tolosano, E.; Beringhelli, T.; Fasano, M. Hemoglobin and heme scavenging. *IUBMB Life* **2005**, *57*, 749–759. [[CrossRef](#)] [[PubMed](#)]
14. Dimitrov, J.D.; Roumenina, L.T.; Doltchinkova, V.R.; Mihaylova, N.M.; Lacroix-Desmazes, S.; Kaveri, S.V.; Vassilev, T.L. Antibodies use heme as a cofactor to extend their pathogen elimination activity and to acquire new effector functions. *J. Biol. Chem.* **2007**, *282*, 26696–26706. [[CrossRef](#)]
15. Roumenina, L.T.; Rayes, J.; Lacroix-Desmazes, S.; Dimitrov, J.D. Heme: Modulator of Plasma Systems in Hemolytic Diseases. *Trends Mol. Med.* **2016**, *22*, 200–213. [[CrossRef](#)]
16. McIntyre, J.A.; Wagenknecht, D.R.; Faulk, W.P. Redox-reactive autoantibodies: Detection and physiological relevance. *Autoimmun. Rev.* **2006**, *5*, 76–83. [[CrossRef](#)]
17. McIntyre, J.A.; Wagenknecht, D.R.; Faulk, W.P. Autoantibodies unmasked by redox reactions. *J. Autoimmun.* **2005**, *24*, 311–317. [[CrossRef](#)]
18. Bozinovic, N.; Noé, R.; Kanyavuz, A.; Lecerf, M.; Dimitrov, J.D. Method for identification of heme-binding proteins and quantification of their interactions. *Anal. Biochem.* **2020**, *607*, 113865. [[CrossRef](#)]
19. Lecerf, M.; Kanyavuz, A.; Rossini, S.; Dimitrov, J.D. Interaction of clinical-stage antibodies with heme predicts their physiochemical and binding qualities. *Commun. Biol.* **2021**, *4*, 391. [[CrossRef](#)]
20. Lin, J.-S.; Lai, E.-M. Protein–Protein Interactions: Co-Immunoprecipitation. In *Bacterial Protein Secretion Systems: Methods and Protocols*; Journet, L., Cascales, E., Eds.; Springer: New York, NY, USA, 2017; pp. 211–219.
21. Chakraborty, A.; Boel, N.M.; Edkins, A.L. HSP90 Interacts with the Fibronectin N-terminal Domains and Increases Matrix Formation. *Cells* **2020**, *9*, 272. [[CrossRef](#)]
22. Pérez-Domínguez, S.; Caballero-Mancebo, S.; Marcuello, C.; Martínez-Júlvez, M.; Medina, M.; Lostao, A. Nanomechanical Study of Enzyme: Coenzyme Complexes: Bipartite Sites in Plastidic Ferredoxin-NADP⁺ Reductase for the Interaction with NADP⁺. *Antioxidants* **2022**, *11*, 537. [[CrossRef](#)] [[PubMed](#)]
23. Marcuello, C.; de Miguel, R.; Lostao, A. Molecular Recognition of Proteins through Quantitative Force Maps at Single Molecule Level. *Biomolecules* **2022**, *12*, 594. [[CrossRef](#)] [[PubMed](#)]
24. Fabian, R.; Gaire, S.; Tyson, C.; Adhikari, R.; Pegg, I.; Sarkar, A. A Horizontal Magnetic Tweezers for Studying Single DNA Molecules and DNA-Binding Proteins. *Molecules* **2021**, *26*, 4781. [[CrossRef](#)] [[PubMed](#)]
25. Zhang, R.; Wang, Y.; Yang, G. DNA–Lysozyme Nanoarchitectonics: Quantitative Investigation on Charge Inversion and Compaction. *Polymers* **2022**, *14*, 1377. [[CrossRef](#)]
26. Rainey, K.H.; Patterson, G.H. Photoswitching FRET to monitor protein–protein interactions. *Proc. Natl. Acad. Sci. USA* **2019**, *116*, 864–873. [[CrossRef](#)]
27. Qiao, Y.; Luo, Y.; Long, N.; Xing, Y.; Tu, J. Single-Molecular Förster Resonance Energy Transfer Measurement on Structures and Interactions of Biomolecules. *Micromachines* **2021**, *12*, 492. [[CrossRef](#)]
28. El Khamlichi, C.; Reverchon-Assadi, F.; Hervouet-Coste, N.; Blot, L.; Reiter, E.; Morisset-Lopez, S. Bioluminescence Resonance Energy Transfer as a Method to Study Protein–Protein Interactions: Application to G Protein Coupled Receptor Biology. *Molecules* **2019**, *24*, 537. [[CrossRef](#)]
29. Fujimoto, A.; Lyu, Y.; Kinjo, M.; Kitamura, A. Interaction between Spike Protein of SARS-CoV-2 and Human Virus Receptor ACE2 Using Two-Color Fluorescence Cross-Correlation Spectroscopy. *Appl. Sci.* **2021**, *11*, 10697. [[CrossRef](#)]

30. Jakobowska, I.; Becker, F.; Minguzzi, S.; Hansen, K.; Henke, B.; Epalle, N.H.; Beitz, E.; Hannus, S. Fluorescence Cross-Correlation Spectroscopy Yields True Affinity and Binding Kinetics of Plasmodium Lactate Transport Inhibitors. *Pharmaceuticals* **2021**, *14*, 757. [\[CrossRef\]](#)
31. Kamal, J.K.; Behere, D.V. Spectroscopic studies on human serum albumin and methemalbumin: Optical, steady-state, and picosecond time-resolved fluorescence studies, and kinetics of substrate oxidation by methemalbumin. *J. Biol. Inorg. Chem.* **2002**, *7*, 273–283. [\[CrossRef\]](#)
32. Ascenzi, P.; di Masi, A.; De Sanctis, G.; Coletta, M.; Fasano, M. Ibuprofen modulates allosterically NO dissociation from ferrous nitrosylated human serum heme-albumin by binding to three sites. *Biochem. Biophys. Res. Commun.* **2009**, *387*, 83–86. [\[CrossRef\]](#)
33. Noé, R.; Bozinovic, N.; Lecerf, M.; Lacroix-Desmazes, S.; Dimitrov, J.D. Use of cysteine as a spectroscopic probe for of heme-scavenging capacity of serum proteins and whole human serum. *J. Pharm. Biomed. Anal.* **2019**, *172*, 311–319. [\[CrossRef\]](#)
34. Leeman, M.; Choi, J.; Hansson, S.; Storm, M.U.; Nilsson, L. Proteins and antibodies in serum, plasma, and whole blood-size characterization using asymmetrical flow field-flow fractionation (AF4). *Anal. Bioanal. Chem.* **2018**, *410*, 4867–4873. [\[CrossRef\]](#)
35. Rambaldi, D.C.; Zattoni, A.; Casolari, S.; Reschiglian, P.; Roessner, D.; Johann, C. An Analytical Method for Size and Shape Characterization of Blood Lipoproteins. *Clin. Chem.* **2007**, *53*, 2026–2029. [\[CrossRef\]](#)
36. Zattoni, A.; Rambaldi, D.C.; Roda, B.; Parisi, D.; Roda, A.; Moon, M.H.; Reschiglian, P. Hollow-fiber flow field-flow fractionation of whole blood serum. *J. Chromatogr. A* **2008**, *1183*, 135–142. [\[CrossRef\]](#)
37. Contado, C. Field flow fractionation techniques to explore the “nano-world”. *Anal. Bioanal. Chem.* **2017**, *409*, 2501–2518. [\[CrossRef\]](#)
38. Marassi, V.; Roda, B.; Zattoni, A.; Tanase, M.; Reschiglian, P. Hollow fiber flow field-flow fractionation and size-exclusion chromatography with MALS detection: A complementary approach in biopharmaceutical industry. *J. Chromatogr. A* **2014**, *1372c*, 196–203. [\[CrossRef\]](#)
39. Marassi, V.; Casolari, S.; Roda, B.; Zattoni, A.; Reschiglian, P.; Panzavolta, S.; Tofail, S.A.M.; Ortelli, S.; Delpivo, C.; Blosi, M.; et al. Hollow-fiber flow field-flow fractionation and multi-angle light scattering investigation of the size, shape and metal-release of silver nanoparticles in aqueous medium for nano-risk assessment. *J. Pharm. Biomed. Anal.* **2015**, *106*, 92–99. [\[CrossRef\]](#)
40. Marassi, V.; Beretti, F.; Roda, B.; Alessandrini, A.; Facci, P.; Maraldi, T.; Zattoni, A.; Reschiglian, P.; Portolani, M. A new approach for the separation, characterization and testing of potential prionoid protein aggregates through hollow-fiber flow field-flow fractionation and multi-angle light scattering. *Anal. Chim. Acta* **2019**, *1087*, 121–130. [\[CrossRef\]](#)
41. Marassi, V.; Mattarozzi, M.; Toma, L.; Giordani, S.; Ronda, L.; Roda, B.; Zattoni, A.; Reschiglian, P.; Careri, M. FFF-based high-throughput sequence shortlisting to support the development of aptamer-based analytical strategies. *Anal. Bioanal. Chem.* **2022**, *414*, 5519–5527. [\[CrossRef\]](#)
42. Wankar, J.; Bonvicini, F.; Benkovics, G.; Marassi, V.; Malanga, M.; Fenyvesi, E.; Gentilomi, G.A.; Reschiglian, P.; Roda, B.; Manet, I. Widening the Therapeutic Perspectives of Clofazimine by Its Loading in Sulfobutylether β -Cyclodextrin Nanocarriers: Nanomolar IC(50) Values against MDR *S. epidermidis*. *Mol. Pharm.* **2018**, *15*, 3823–3836. [\[CrossRef\]](#) [\[PubMed\]](#)
43. Ventouri, I.K.; Loeber, S.; Somsen, G.W.; Schoenmakers, P.J.; Astefanei, A. Field-flow fractionation for molecular-interaction studies of labile and complex systems: A critical review. *Anal. Chim. Acta* **2022**, *1193*, 339396. [\[CrossRef\]](#)
44. Reschiglian, P.; Rambaldi, D.C.; Zattoni, A. Flow field-flow fractionation with multiangle light scattering detection for the analysis and characterization of functional nanoparticles. *Anal. Bioanal. Chem.* **2011**, *399*, 197–203. [\[CrossRef\]](#)
45. Marassi, V.; Di Cristo, L.; Smith, S.G.J.; Ortelli, S.; Blosi, M.; Costa, A.L.; Reschiglian, P.; Volkov, Y.; Prina-Mello, A. Silver nanoparticles as a medical device in healthcare settings: A five-step approach for candidate screening of coating agents. *R. Soc. Open Sci.* **2018**, *5*, 171113. [\[CrossRef\]](#)
46. Marassi, V.; Casolari, S.; Panzavolta, S.; Bonvicini, F.; Gentilomi, G.A.; Giordani, S.; Zattoni, A.; Reschiglian, P.; Roda, B. Synthesis Monitoring, Characterization and Cleanup of Ag-Polydopamine Nanoparticles Used as Antibacterial Agents with Field-Flow Fractionation. *Antibiotics* **2022**, *11*, 358. [\[CrossRef\]](#)
47. Roda, B.; Marassi, V.; Zattoni, A.; Borghi, F.; Anand, R.; Agostoni, V.; Gref, R.; Reschiglian, P.; Monti, S. Flow field-flow fractionation and multi-angle light scattering as a powerful tool for the characterization and stability evaluation of drug-loaded metal-organic framework nanoparticles. *Anal. Bioanal. Chem.* **2018**, *410*, 5245–5253. [\[CrossRef\]](#)
48. Marassi, V.; Calabria, D.; Trozzi, I.; Zattoni, A.; Reschiglian, P.; Roda, B. Comprehensive characterization of gold nanoparticles and their protein conjugates used as a label by hollow fiber flow field flow fractionation with photodiode array and fluorescence detectors and multiangle light scattering. *J. Chromatogr. A* **2021**, *1636*, 461739. [\[CrossRef\]](#)
49. Marassi, V.; Maggio, S.; Battistelli, M.; Stocchi, V.; Zattoni, A.; Reschiglian, P.; Guescini, M.; Roda, B. An ultracentrifugation–hollow-fiber flow field-flow fractionation orthogonal approach for the purification and mapping of extracellular vesicle subtypes. *J. Chromatogr. A* **2021**, *1638*, 461861. [\[CrossRef\]](#)
50. Marassi, V.; De Marchis, F.; Roda, B.; Bellucci, M.; Capecchi, A.; Reschiglian, P.; Pompa, A.; Zattoni, A. Perspectives on protein biopolymers: Miniaturized flow field-flow fractionation-assisted characterization of a single-cysteine mutated phaseolin expressed in transplastomic tobacco plants. *J. Chromatogr. A* **2021**, *1637*, 461806. [\[CrossRef\]](#)
51. Marassi, V.; Marangon, M.; Zattoni, A.; Vincenzi, S.; Versari, A.; Reschiglian, P.; Roda, B.; Curioni, A. Characterization of red wine native colloids by asymmetrical flow field-flow fractionation with online multidetection. *Food Hydrocoll.* **2021**, *110*, 106204. [\[CrossRef\]](#)

-
52. Marassi, V.; Roda, B.; Casolari, S.; Ortell, S.; Blois, M.; Zattoni, A.; Costa, A.L.; Reschiglian, P. Hollow-fiber flow field-flow fractionation and multi-angle light scattering as a new analytical solution for quality control in pharmaceutical nanotechnology. *Microchem. J.* **2018**, *136*, 149–156. [[CrossRef](#)]
53. Reschiglian, P.; Roda, B.; Zattoni, A.; Tanase, M.; Marassi, V.; Serani, S. Hollow-fiber flow field-flow fractionation with multi-angle laser scattering detection for aggregation studies of therapeutic proteins Field-Flow Fractionation. *Anal. Bioanal. Chem.* **2014**, *406*, 1619–1627. [[CrossRef](#)] [[PubMed](#)]
54. Zhao, E.J.; Carruthers, M.N.; Li, C.H.; Mattman, A.; Chen, L.Y.C. Conditions associated with polyclonal hypergammaglobulinemia in the IgG4-related disease era: A retrospective study from a hematology tertiary care center. *Haematologica* **2020**, *105*, e121. [[CrossRef](#)] [[PubMed](#)]
55. Ross, J.R. Practical Handbook of Biochemistry and Molecular Biology: Edited by G D Fasman. pp 601. CRC Press: Boca Raton, Florida, USA. 1989. \$00 ISBN 0-8493-3705-4. *Biochem. Educ.* **1991**, *19*, 95–96. [[CrossRef](#)]
56. Abbate, R.A.; Raak, N.; Boye, S.; Janke, A.; Rohm, H.; Jaros, D.; Lederer, A. Asymmetric flow field flow fractionation for the investigation of caseins cross-linked by microbial transglutaminase. *Food Hydrocoll.* **2019**, *92*, 117–124. [[CrossRef](#)]
57. Karnaukhova, E.; Owczarek, C.; Schmidt, P.; Schaer, D.J.; Buehler, P.W. Human Plasma and Recombinant Hemopexins: Heme Binding Revisited. *Int. J. Mol. Sci.* **2021**, *22*, 1199. [[CrossRef](#)]
58. Rivas-Urbina, A.; Rull, A.; Aldana-Ramos, J.; Santos, D.; Puig, N.; Farre-Cabrerizo, N.; Benitez, S.; Perez, A.; de Gonzalo-Calvo, D.; Escola-Gil, J.C.; et al. Subcutaneous Administration of Apolipoprotein J-Derived Mimetic Peptide d-[113–122]apoJ Improves LDL and HDL Function and Prevents Atherosclerosis in LDLR-KO Mice. *Biomolecules* **2020**, *10*, 829. [[CrossRef](#)]
59. Alouffi, S.; Faisal, M.; Alatar, A.A.; Ahmad, S. Oxidative Modification of LDL by Various Physicochemical Techniques: Its Probable Role in Diabetes Coupled with CVDs. *BioMed Res. Int.* **2018**, *2018*, 7390612. [[CrossRef](#)]
60. Gorshkova, E.N.; Lecerf, M.; Astrakhantseva, I.V.; Vasilenko, E.A.; Starkina, O.V.; Ilyukina, N.A.; Dimitrova, P.A.; Dimitrov, J.D.; Vassilev, T.L. Induced antigen-binding polyreactivity in human serum IgA. *Immunobiology* **2022**, *227*, 152213. [[CrossRef](#)]
61. Hart, F.; Danielczyk, A.; Goletz, S. Human Cell Line-Derived Monoclonal IgA Antibodies for Cancer Immunotherapy. *Bioengineering* **2017**, *4*, 42. [[CrossRef](#)]
62. Gbotosho, O.T.; Kapetanaki, M.G.; Kato, G.J. The Worst Things in Life are Free: The Role of Free Heme in Sickle Cell Disease. *Front. Immunol.* **2021**, *11*, 561917. [[CrossRef](#)] [[PubMed](#)]